Fabrication and Characterization of High-Quality Uniform and Apodized Si_3N_4 Waveguide Gratings Using Laser Interference Lithography

W. C. L. Hopman, *Student Member, IEEE*, R. Dekker, *Student Member, IEEE*, D. Yudistira, *Student Member, IEEE*, W. F. A. Engbers, H. J. W. M. Hoekstra, and R. M. de Ridder, *Member, IEEE*

***Abstract*—A method is presented for fabricating high-quality ridge waveguide gratings by combining conventional mask lithography with laser interference lithography. The method, which allows for apodization functions modulating both amplitude and phase of the grating is demonstrated by fabricating a grating that is chirped by width-variation of the grated ridge waveguide. The structure was optically characterized using both an end-fire and an infrared camera setup to measure the transmission and to map and quantify the power scattered out of the grating, respectively. For a uniform grating, we found a Q value of $\sim$8000 for the resonance peak near the lower wavelength band edge, which was almost completely suppressed after apodization.**

***Index Terms*—Electromagnetic scattering by periodic structures, gratings, optical device fabrication, optical waveguide filters, ridge waveguides.**

I. Introduction

WAVEGUIDE gratings (WGGs) have shown their value for many years in filters and mirrors [1], sensors [2], lasers [3], second-harmonic generation [4], tunable time-delays [5], and many more applications and theoretical studies. In a WGG, a guided mode is manipulated through a one-dimensional periodic variation of the dielectric constant along the propagation direction. An important property of finite uniform periodic structures in lossless media is the occurrence of fringes in the transmission and reflection spectra near the stopband edges. It is well known that these oscillations in the transfer function (near the edges outside the stopband) of a uniform grating are due to Fabry–Pérot resonance modes of the grating Bloch modes [6]. These fringes which are undesired for many applications, e.g., wavelength filtering, can be strongly reduced by apodization, i.e., making gradual transitions between the grating region and the unperturbed waveguide [7]. The optimum shape of the apodization function depends on the application and the grating parameters, and in general requires numerical optimization [8]–[10]. In this letter, we propose a fabrication scheme which provides a straightforward way of implementing two types of apodization: 1) chirping through varying the width of the ridge-WGG [11], [12], and 2) strength modulation by varying the width or location of the grating [12]. The main difference of our approach compared to most other approaches known from literature, e.g., [9], [10], [13], is that we first pattern the waveguides and the apodization function using conventional UV lithography, and then use laser interference lithography (LIL) [14] in combination with an image reversal bake for defining the grating with the desired shape. In this letter, we will show that these relatively strong low-loss WGGs can have a high quality factor for a first-order longitudinal Fabry–Pérot resonance in the case of no apodization. We demonstrate the potential of our fabrication method only for the chirp-based apodization method, because of its larger misalignment tolerance. We did not attempt to optimize the apodization function, but just chose to linearly taper the waveguide width to chirp the effective index. This led to an evident reduction of the fringes near the lower wavelength side of the stopband edge. This is shown by both transmission and scatter measurements using an end-fire and an infrared-camera setup [15], respectively.

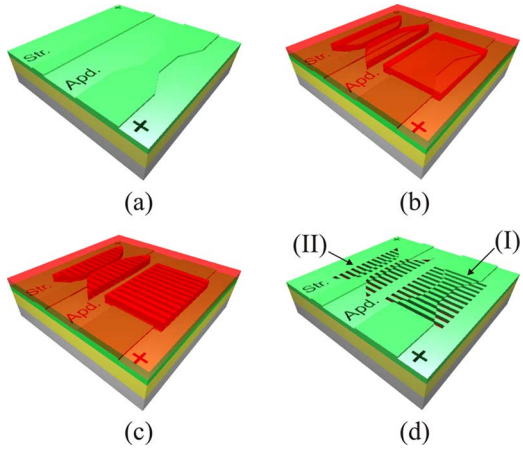

Fig. 1. Schematic representation of the triple step lithographic fabrication process of the grated ridge waveguides. (Color version available online at http://ieeexplore.ieee.org.)

II. Realization

The fabrication of the grated ridge waveguide structures consisted of a three-step etching process performed on a Si_3N_4 guiding layer. First, a 275-nm-thick stoichiometric Si_3N_4 ($n = 1.981$) slab was deposited on an 8-μm thermally grown SiO_2 ($n = 1.445$) buffer, using low-pressure chemical

Manuscript received February 8 2006; revised June 8, 2006. This work was supported by NanoNed, a national nanotechnology program, and by the Freeband Impuls Program, both coordinated by the Dutch Ministry of Economic Affairs, and also by the Dutch Technology Foundation STW.

The authors are with the Mesa+ Research Institute, University of Twente, 7500 AE Enschede, The Netherlands (e-mail: w.c.l.hopman@utwente.nl).

Digital Object Identifier 10.1109/LPT.2006.881226

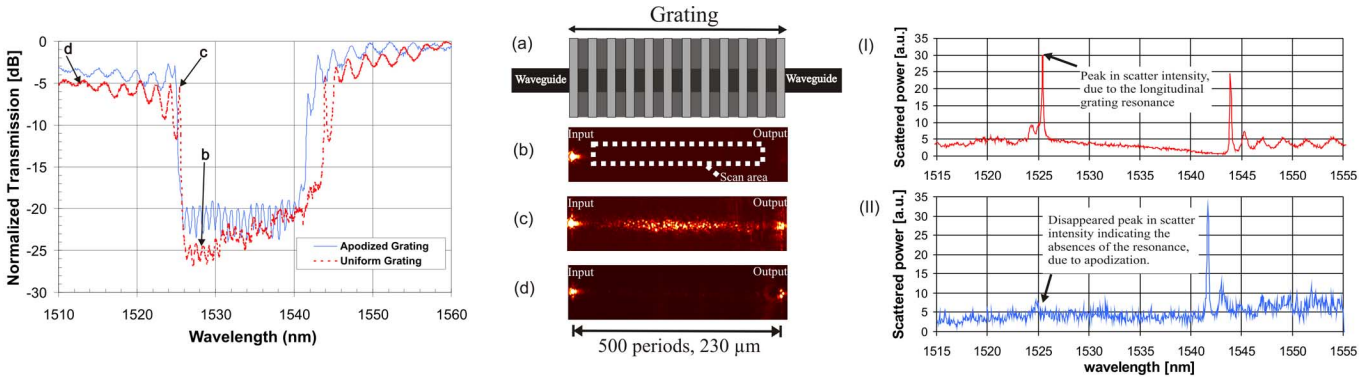

Fig. 2. Optical characterization of the fabricated gratings. Left: Measured transmission of the uniform (dashed) and apodized (solid) gratings, showing less pronounced fringes in the short-wavelength transmission band for the apodized case. The oscillations in the stopband at low transmitted power, are caused by a parasitic Fabry–Pérot effect in the sample. Middle (uniform grating without cladding): (a) Schematic top view (grating period exaggerated); (b) no power transmission in the stopband. The dotted contour indicates the area from which scattered light was collected to produce the right-hand graphs (I) and (II); (c) full transmission at the first resonance mode (see label c in the left graph), exhibiting strongly enhanced scattering in the grated region; (d) full transmission outside the stopband, almost without increased scattering in the grating region. Right: Light scattered out of the grating region within the dotted contour in (b); (I) uniform grating showing two distinct peaks at the band edge positions; (II) apodized grating showing almost complete suppression of the short-wavelength peak. (Color version available online at http://ieeexplore.ieee.org.)

vapor deposition. The first mask (darkfield) contained text comments and alignment markers to assist further processing and characterization. This pattern was etched completely through the guiding film using a reactive ion etching (RIE) process. A second mask (brightfield) defining both waveguide and taper structures was used for patterning the ridge waveguides. Our waveguide design called for a 5-nm ridge step, which was achieved [Fig. 1(a)] after exposing the Si_3N_4 slab to buffered HF for 7 min. The gratings were defined using LIL, a technique that typically exposes a much larger area (several centimeters squared) than needed for the gratings. In order to confine the gratings and to define the apodization functions, a positive image reversal resist (Ti04-TX from MicroChemicals) was used with a double exposure technique.

The first exposure for 5.5 s through a third (bright-field) mask defined the grating areas. After an image reversal bake, all areas where no grating was desired became insoluble and insensitive to further exposure, while the photosensitivity of the future grating areas was preserved Fig. 1(b). The second exposure was made using a Lloyd's mirror LIL setup [14] employing a laser wavelength of 266 nm to realize $\Lambda = 460$ nm period gratings having a duty cycle of 20% [Fig. 1(c)]. Finally, the gratings were transferred to the Si_3N_4-layer using RIE [Fig. 1(d)]. An etch depth of 60 nm was estimated using both profilometry and fitting of optical measurement data using a mode expansion technique. Finally, a polymer top cladding ($n \approx 1.5$) was applied to the grating regions for ensuring single-mode behavior.

III. Realization of Apodization Functions

As mentioned in the introduction, two types of apodization can be achieved using our scheme, i.e., 1) chirping and 2) strength modulation. The first method uses a variation of the waveguide width to obtain a corresponding position-dependent variation of the modal propagation constant [Fig. 1(d-I)]. Thus, the mode has a position-dependent tuning with respect to the grating constant $2\pi/\Lambda$, having an effect equivalent to a period-chirped grating. Since this chirping function is determined by the local waveguide width, its realization process is essentially self-aligned and the definition of the grating areas only requires coarse alignment. The second method varies the effective grating strength by varying the overlap of the grating with the waveguide modal field. By positioning the lateral grating edge in the evanescent modal field tail [Fig. 1(d-II)], the effective grating strength can be gradually increased, starting from zero without the need for high resolution lithography, allowing, e.g., the realization of the well-known raised cosine function [12]. The methods could be combined in order to modulate both the phase and the amplitude of the grating.

We chose to use only Method 1 with a three-section linearly tapered waveguide (Section 1: 7–2 μm over 225 periods; Section 2: 50 periods at 2 μm width; Section 3: inverse of Section 1), which certainly does not result in an optimum apodization function, but which serves our purpose of demonstrating the technology. Modeling results showed that this type of apodization resulted in a reduction of the group delay (resonances) at the short-wavelength side of the stopband [6], which is experimentally verified in Section V.

IV. Experimental Setup

Both an end-fire setup and an infrared (IR)-sensitive camera were used for characterizing the WGGs. The IR camera was positioned to collect the scattered photons from a selected area of the grating [see the dotted rectangle in middle graph of Fig. 2(b)]. For the analyses, we assume that the Rayleigh scattering is proportional to the local intensity. The available 12-bit IR camera produced images of 320×240 pixels, each pixel representing a 0.8 μm$\times$ 0.8 μm chip area. The WGGs show a relatively small amount of scattering (compared to the peak value at resonance) at wavelengths outside the stopband, except for the transitions at the beginning and end of the grating. This low amount of scattering gives a clear indication of a high quality (e.g., low roughness) of the fabricated device and also leads to a fully exploited dynamic range of the IR-camera indicated by the graphs in Fig. 2(right).

For the end-fire transmission experiments, we coupled light into the TE_{00} waveguide mode using a tunable laser

(1470–1580 nm) in combination with a polarization controller. Since our photodetector was calibrated and the transmission graph of the waveguides showed a flat spectrum, we omitted further normalization.

V. Experimental Results

The transmission results of WGGs, both with (solid curve) and without (dotted) apodization are shown in Fig. 2(left). The nonapodized structure shows sharp fringes at the left edge of the stopband, of which especially the first one is significantly reduced in the apodized case, as expected [6]. A slightly reduced stopband is observed induced by the apodization. The middle part of Fig. 2 shows three camera frames of the uniform grating but without cladding, taken at different wavelengths, see the labels in the left graph: in the stopband (b); at the first fringe (c); outside the stopband (d). The input and output of the grating can easily be distinguished by the relatively high scattering from these spots. The envelope of the scattering intensity of the first resonance perfectly matches the first-order Fabry–Pérot-like resonance of the Bloch modes in the grating [4]. The quality Q-factor, defined as the ratio between the wavelength and the -3-dB bandwidth of the resonance peak, can be obtained both from the scatter graph Fig. 2(right)] and the transmission spectrum [Fig. 2(left)]. For both cases, we find $Q \approx 8000$. With an air cladding, $Q \approx 14000$ is found. These numbers give an indication of the experienced optical loss that is induced by for example nonuniformities in etch depth, layer thickness, waveguide width, material loss, etc.

A clear evidence of a successful reduction of the first-order grating resonance is shown in the right part of Fig. 2. The upper graph (I) shows the integrated collected scatter intensity for the uniform grating. Near the stopband edges there is a huge increase in scatter intensity. It has been shown that these resonances can be used for integrated sensors [2]. However, these high-Q resonances, corresponding to large group delays [5], limit the bandwidth for the use in telecom applications. Furthermore, the apodized structure (II) shows an almost total disappearance of the previously mentioned resonance on the left side of the stopband, which indicates strongly reduced group delays. Further modeling suggests that an even larger sidelobe reduction can be achieved by using a slightly larger ridge height (e.g., 10 nm), though its impact on fabrication processes should be taken into account carefully.

VI. Conclusion

WGGs have successfully been realized in Si_3N_4 using a complementary metal–oxide–semiconductor compatible technology by combining both conventional and LIL. A strongly increased amount of scattering was observed for a wavelength near the stopband edge in the grating region using an IR camera, indicating a large group delay. Quality factors of 8000 and 14 000 were observed for resonances in uniform gratings with and without a polymer cladding, respectively. The reduction of some of the Fabry–Pérot-like resonances outside the stopband of the grating, indicating a strong reduction of the group delay, has been achieved by a width-tapering scheme, as observed from both the transmission and scatter measurement data. This demonstrates that in principle our method is suitable for implementing apodization functions.

References

[1] J. F. Lepage, R. Massudi, G. Anctil, S. Gilbert, M. Piche, and N. McCarthy, "Apodizing holographic gratings for the modal control of semiconductor lasers," *Appl. Opt.*, vol. 36, pp. 4993–4998, 1997.

[2] W. C. L. Hopman, P. Pottier, D. Yudistira, J. van Lith, P. V. Lambeck, R. M. De La Rue, A. Driessen, H. Hoekstra, and R. M. de Ridder, "Quasi-one-dimensional photonic crystal as a compact building-block for refractometric optical sensors," *IEEE J. Sel. Topics Quantum Electron.*, vol. 11, no. 1, pp. 11–16, Jan./Feb. 2005.

[3] P. Madasamy, G. N. Conti, P. Poyhonen, Y. Hu, M. M. Morrell, D. F. Geraghty, S. Honkanen, and N. Peyghambarian, "Waveguide distributed Bragg reflector laser arrays in erbium doped glass made by dry Ag film ion exchange," *Opt. Eng.*, vol. 41, pp. 1084–1086, 2002.

[4] D. Faccio, F. Bragheri, and M. Cherchi, "Optical Bloch-mode-induced quasi-phase matching of quadratic interactions in one-dimensional photonic crystals," *J. Opt. Soc. Amer. B*, vol. 21, pp. 296–301, 2004.

[5] M. L. Povinelli, S. G. Johnson, and J. D. Joannopoulos, "Slow-light, band-edge waveguides for tunable time delays," *Opt. Express*, vol. 13, pp. 7145–7159, 2005.

[6] J. E. Sipe, L. Poladian, and C. M. de Sterke, "Propagation through nonuniform grating structures," *J. Opt. Soc. Amer. A*, vol. 11, pp. 1307–1307, 1994.

[7] M. Matsuhara and K. O. Hill, "Optical-waveguide band-rejection filters: Design," *Appl. Opt.*, vol. 13, pp. 2886–2888, 1974.

[8] K. Ennser, N. Zervas, and R. L. Laming, "Optimization of apodized linearly chirped fiber gratings for optical communications," *IEEE J. Quantum Electron.*, vol. 34, no. 5, pp. 770–778, May 1998.

[9] D. Wiesmann, C. David, R. Germann, D. Emi, and G. L. Bona, "Apodized surface-corrugated gratings with varying duty cycles," *IEEE Photon. Technol. Lett.*, vol. 12, no. 6, pp. 639–641, Jun. 2000.

[10] T. W. Mossberg, C. Greiner, and D. Iazikov, "Interferometric amplitude apodization of integrated gratings," *Opt. Express*, vol. 13, pp. 2419–2426, 2005.

[11] H. Abe, S. G. Ayling, J. H. Marsh, R. M. de la Rue, and J. S. Roberts, "Single-mode operation of a surface grating distributed-feedback Gaas-Algaas laser with variable-width wave-guide," *IEEE Photon. Technol. Lett.*, vol. 7, no. 5, pp. 452–454, May 1995.

[12] J. T. Hastings, M. H. Lim, J. G. Goodberlet, and H. I. Smith, "Optical waveguides with apodized sidewall gratings via spatial-phase-locked electron-beam lithography," *J. Vac. Sci. Technol. B*, vol. 20, pp. 2753–2757, 2002.

[13] C. T. Brooks, G. L. Vossler, and K. A. Winick, "Integrated-optic dispersion compensator that uses chirped gratings," *Opt. Lett.*, vol. 20, pp. 368–370, 1995.

[14] F. J. van Soest, H. van Wolferen, H. Hoekstra, R. M. de Ridder, K. Worhoff, and P. V. Lambeck, "Laser interference lithography with highly accurate interferometric alignment," *Jpn. J. Appl. Phys.*, vol. 44, pt. 1, pp. 6568–6570, 2005.

[15] S. J. McNab, N. Moll, and Y. A. Vlasov, "Ultra-low loss photonic integrated circuit with membrane-type photonic crystal waveguides," *Opt. Express*, vol. 11, pp. 2927–2939, 2003.